

# Characterization of isolated photosystem I from *Halomicronema hongdechloris*, a chlorophyll *f*-producing cyanobacterium

Y. LI, N. VELLA, and M. CHEN<sup>+</sup>

*School of Life and Environmental Science, University of Sydney, NSW 2006, Australia*

## Abstract

*Halomicronema hongdechloris* is a chlorophyll (Chl) *f*-producing cyanobacterium. Chl *f* biosynthesis is induced under far-red light, extending its photosynthetically active radiation range to 760 nm. In this study, PSI complexes were isolated and purified from *H. hongdechloris*, grown under white light (WL) and far-red light (FR), by a combination of density gradient ultracentrifugation and chromatographic separation. WL-PSI showed similar pigment composition as that of *Synechocystis* 6803, using Chl *a* in the reaction center. Both Chl *a* and *f* were detected in the FR-PSI, although Chl *f* was a minor component (~8% of total Chl). The FR-PSI showed a maximal fluorescence emission peak of 750 nm at 77 K, which is red-shifted ~20 nm compared to the 730 nm recorded from the WL-PSI. The absorption peaks of P700 for WL-PSI and FR-PSI were 699 nm and 702 nm, respectively. The function of Chl *f* in FR-PSI is discussed.

*Additional key words:* cyanobacteria; far-red light photoacclimation; oxygenic photosynthesis; red-shifted chlorophyll.

## Introduction

Cyanobacteria, green algae and plants perform oxygenic photosynthesis, which converts solar energy to chemical energy resulting in the estimated creation of more than 100 billion tons of dry biomass per year (Hou *et al.* 2014, Nelson and Junge 2015). This process relies on the cooperative interaction of two photosystems, PSI and PSII. When light is absorbed by oxygenic photosynthetic organisms, PSII generates a very high oxidizing power that is sufficient to split water and produce molecular oxygen (Barber 2008). In contrast, PSI provides the reductant to reduce NADP<sup>+</sup> to NADPH through the linear electron transfer chain from PSII to PSI (Fromme *et al.* 2001, Croce and van Amerongen 2013, El-Khouly *et al.* 2017).

Higher plant PSI exists as a monomeric form, but in cyanobacteria, most PSI exists in a trimeric form (Jordan *et al.* 2001, Ben-Shem *et al.* 2003, Amunts *et al.* 2010). Typical PSI complexes of cyanobacteria consist of 12 different protein subunits, including 9 transmembrane subunits (PsaA, PsaB, PsaF, PsaI, PsaJ, PsaK, PsaL, PsaM,

and PsaX) and three membrane extrinsic subunits (PsaC, PsaD, PsaE) (Jordan *et al.* 2001). These proteins bind with 127 cofactors including 96 chlorophylls, 22 carotenoids, 2 phylloquinones, and 3 iron-sulfur clusters (Fe<sub>4</sub>S<sub>4</sub>) to perform light capturing and electron transfer in PSI (Jordan *et al.* 2001). The heterodimer of PsaA and PsaB forms the reaction center core of PSI proteins (about 83 kDa) (Golbeck 1994, Jordan *et al.* 2001). The central domains of the PsaA and PsaB subunits form interlocked semicircles and are coordinated to the special pair of Chl *a* (P700) as primary electron donor (Jordan *et al.* 2001, Golub *et al.* 2017). PsaC, PsaD, and PsaE are three subunits exposed to the stromal side, and together form the docking site for iron-sulfur centers and ferredoxin (Barth *et al.* 1998, Xu *et al.* 2003, Grotjohann and Fromme 2005, El-Mohsnawy *et al.* 2010). PsaL, PsaI, and PsaM are found at the interface between the PSI monomers in the trimeric PSI complexes, which are absent in plants (Grotjohann and Fromme 2005). PsaL forms the connection domain to link

Received 21 September 2017, accepted 15 November 2017, published as online-first 10 January 2018.

<sup>+</sup>Corresponding author; e-mail: [min.chen@sydney.edu.au](mailto:min.chen@sydney.edu.au)

**Abbreviations:** APC – allophycocyanin; CCA – complementary chromatic adaptation; Chl – chlorophyll; FR – 730 nm light-emitting diodes; DoDM –  $\beta$ -dodecyl maltoside; FaRLiP – far-red light photoacclimation; FR – far-red light; FR-PSI – isolated PSI from 730 nm LED-illuminated culture; OG – *n*-octyl- $\beta$ -D-glucopyranoside; PC – phycocyanin; TMPD – N,N,N',N'-tetramethyl-*p*-phenylenediamine; WL – white fluorescent light; WL-PSI – isolated PSI from white light culture; 6803-PSI – purified PSI complexes from *Synechocystis* 6803.

**Acknowledgements:** The research was supported by the Australian Research Council Centre of Excellence for translational photosynthesis (CE140100015). The authors thank Dr. Ben Crossette (mass-spectral facility, University of Sydney) and Dr. Miguel A. Hernández-Prieto for assisting with LC-MS/MS and spectral analysis.

the PSI monomers, and the PsaI and PsaM nearby also contribute to the stability of PSI trimers (Xu *et al.* 1995, Schluchter *et al.* 1996, Mühlenhoff *et al.* 1996, Grotjohann and Fromme 2005). Recently, a new type of PsaL is reported for the formation of tetrameric and dimeric PSI in the thermophilic cyanobacterium *Chroococcidiopsis* sp. TS-821 (Li *et al.* 2014). Four small subunits PsaF, PsaJ, PsaK, and PsaX are located at the distal side of the PSI complexes and may be responsible for stabilizing the core antenna system of PSI. They may also be involved in the interaction of PSI with its external antenna systems, such as IsiA or phycobilisomes (Grotjohann and Fromme 2005).

Typically, the P700 special pair is composed of a hetero-dimeric form of a Chl *a* and a Chl *a'* (C13 epimer of Chl *a*) (Jordan *et al.* 2001). Chl *a* is the only chlorophyll that is a primary electron donor in PSI, with an exception found in *Acaryochloris marina* (*A. marina*), a Chl *d*-containing cyanobacterium (Miyashita *et al.* 1996). In *A. marina*, Chl *d* is the dominant pigment and forms the special pair in PSI, P740. It was defined based on its absorption, even though the protein subunit composition of PSI in *A. marina* resembles that of the known PSI complexes from cyanobacteria (Hu *et al.* 1998, Sivakumar *et al.* 2003, Tomo *et al.* 2008). A highly purified PSI complex comprises ~97 Chl *d*, ~2 Chl *a'*, ~25  $\beta$ -carotenes, and 2 phylloquinone molecules per P740 (Tomo *et al.* 2008).

Chl *f* is the most red-shifted of all known Chl with absorption at 707 nm in methanol (Chen *et al.* 2010) and its biosynthesis is reversibly induced by far-red light (FR) (Akutsu *et al.* 2011, Chen *et al.* 2012). Consequently, Chl *f*-containing organisms are able to extend their photosynthetically active absorption range further into the

infrared wavelength region up to 760 nm (Chen and Blankenship 2011, Li *et al.* 2013, Li *et al.* 2015). Chl *f* was proposed to function as an accessory pigment for light harvesting and energy transfer based on its FR-inducible biosynthesis (Akutsu *et al.* 2011, Chen *et al.* 2012).

*H. hongdechloris* synthesizes Chl *f* under FR culture conditions, with Chl *f* comprising up to 15% of total Chl (Chen *et al.* 2012, Li *et al.* 2014). Chl *a* remains the predominant Chl even under different light conditions (Li *et al.* 2014). *H. hongdechloris* has also developed a novel complementary chromatic adaptation (CCA) strategy, using phycobilisomes containing allophycocyanin (APC) and phycocyanin (PC) under WL culture conditions, but using red-shifted APC only under FR culture conditions (Li *et al.* 2016). This novel CCA strategy agrees well with the far-red light photoacclimation (FaRLiP) phenomenon reported in other Chl *f*-producing cyanobacteria (Gan and Bryant 2015). Several cyanobacteria have been identified that can grow photoautotrophically in FR conditions and synthesize Chl *f*, including *H. hongdechloris* (Akutsu *et al.* 2011, Chen *et al.* 2012, Li *et al.* 2014, Airs *et al.* 2014, Gan *et al.* 2014, Gan and Bryant 2015, Ohkubo and Miyashita 2017). Those strains are broadly distributed in different taxonomic sections of cyanobacteria (Gan and Bryant 2015, Li *et al.* 2015). However, the location and function of Chl *f* in the photosynthetic apparatus (light-harvesting complexes and/or reaction centers) remains unknown.

In this study, we purified the PSI complex from *H. hongdechloris* and compared the differences between WL-PSI containing only Chl *a* from WL-grown cultures and the FR-PSI containing Chl *a* and *f* from FR-grown cultures. The function of Chl *f* in isolated PSI is discussed.

## Materials and methods

**Algal culture and thylakoid membrane preparation:** *H. hongdechloris* cells were cultured in modified K+ES seawater media at 32°C under illumination using either 730 nm light-emitting diodes (FR) or white fluorescent light (WL) at the light intensity of 15–20  $\mu$ E (Li *et al.* 2014). *Synechocystis* 6803 was cultured in BG-11 fresh water media under WL illumination at light intensity of 60–100  $\mu$ E.

Cells were harvested at their late log phase by centrifugation and rinsed twice in a buffer containing 20 mM MES-NaOH (pH 6.5), 10 mM CaCl<sub>2</sub>, 10 mM MgCl<sub>2</sub>, 0.5 M mannitol, and 1 mM phenylmethylsulfonyl fluoride (buffer A). Harvested cells were resuspended in the buffer A and broken by a bead-beater with 0.1 mm silica beads using eight cycles of 30 s with 5-min intervals in an ice box. Unbroken cells and debris were removed by centrifuging at 1,000  $\times$  g for 10 min. The supernatant was centrifuged at 30,000  $\times$  g for 30 min to collect the thylakoid membrane fragments. The thylakoid membrane pellets were rinsed with the buffer A several times until no visible blue phycobiliproteins remained in the supernatant. The thylakoid membranes free of phycobiliproteins were

resuspended in the buffer A at Chl *a* concentration of 0.8–1.0 mg ml<sup>-1</sup>.

**Isolation and purification of PSI:** The isolated thylakoid membranes were solubilized using a detergent mixture of 0.8% (w/v)  $\beta$ -dodecyl maltoside (DoDM) and 0.2% *n*-octyl- $\beta$ -D-glucopyranoside (OG) for 1 h in the dark at 4°C. The non-solubilized thylakoid membrane debris was pelleted by centrifugation at 30,000  $\times$  g for 30 min at 4°C. The solubilized protein complexes were separated on a 6-step sucrose gradient [5, 10, 15, 20, 25, and 30% (w/v)] containing 0.02% DoDM and buffer A at 150,000  $\times$  g for at least 16 h at 4°C (*SW 40Ti*, Beckman). The Chl-binding bands were collected by a syringe.

The collected PSI-enriched green band from the sucrose gradient was subsequently purified on an anion exchange column (*Mono Q<sup>TM</sup> 5/50 GL*, GE Healthcare Life Sciences) in the buffer A containing 0.02% DoDM and eluted using the salt gradient of 5–200 mM MgSO<sub>4</sub> at a flow rate of 0.8 ml min<sup>-1</sup>. The major green fractions were collected and further purified using *BioSep SEC s2000* (300 mm  $\times$  4.6 mm, Phenomenex) in the buffer A

containing 0.02% DoDM at a flow rate of 0.2 ml min<sup>-1</sup>.

**Spectral analysis:** Absorption spectral analyses were performed using a *Shimadzu UV-VIS 2550* spectrophotometer at room temperature. Steady-state fluorescence spectral analysis was performed at 77 K using a *Varian Cary Eclipse* fluorescence spectrophotometer with the aid of a cryostat attachment (*Oxford Instruments*). The samples were adjusted to a maximum absorbance of  $\leq 0.1$  for fluorescence measurements in the buffer A containing 65% (v/v) glycerol. The fluorescence spectra were recorded at an average of 50 repeated readings and smoothed by the *Savitzky–Golay* method with window of 10 using *Origin* software (*version 9.0*).

**Pigment composition:** Pigments were extracted from the isolated Chl-binding protein complexes by adding 2-butanol and 4.0 M NaCl to the pigments in a ratio of  $V_{\text{sample}}:V_{\text{butanol}}:V_{\text{NaCl}} = 2:3:1$ . The green-colored butanol phase was collected and 20  $\mu\text{l}$  was immediately injected into high performance liquid chromatography (HPLC) for pigment analysis. HPLC analysis was conducted using a reverse phase C12 column (*Synergi 4u MAX-RP 80A*, 150 mm  $\times$  4.60 mm, *Phenomenex*) at a flow rate of 1 ml min<sup>-1</sup>. The column was equilibrated using solvent A (85% methanol containing 50 mM ammonia acetate) and then run with a linear gradient of solvent A to solvent B (100% methanol) for 8 min, followed by 100% solvent B for 30 min. Eluted pigments were detected with a photodiode array detector (*SPD-M10Avp*, *Shimadzu*) at a range of 370–800 nm. The ratio of isolated pigments was calculated based on HPLC chromatogram peak area at their published extinction coefficients wavelength. The molar extinction coefficients ( $\epsilon$ ) of different pigments in methanol used in this paper were:  $\epsilon = 70.02 \times 10^3$  [L mol<sup>-1</sup> cm<sup>-1</sup>] at 665 nm for Chl *a* (Li *et al.* 2012), Chl *a'* and oxidized Chl *a* used the same  $\epsilon$  as Chl *a*;  $\epsilon = 71.11 \times 10^3$  [L mol<sup>-1</sup> cm<sup>-1</sup>] at 707 nm for Chl *f* (Li *et al.* 2012);  $\epsilon = 141 \times 10^3$  [L mol<sup>-1</sup> cm<sup>-1</sup>] at 453 nm for  $\beta$ -carotene in 100% ethanol (Goodwint *et al.* 1960).

**The polypeptide composition of isolated PSI:** Polypeptide composition of the PSI complexes was resolved by a *Bolt*<sup>TM</sup> 4–12% Bis-Tris PreCast gel using MES-SDS running buffer (*Thermo Fisher Scientific*). Protein samples

## Results

**Purification of PSI:** The PSI-enriched fraction was isolated using sucrose density gradient centrifugation. The *Synechocystis* 6803 grown under WL illumination was used as a control. Two green bands were well resolved from the *H. hongdechloris* samples, assigned as WL-1, WL-2, and FR-1 and FR-2 (Fig. 1A). Two green fractions were also well resolved from *Synechocystis* 6803 and the top part of the density gradients demonstrated a pinkish

were precipitated by adding 10% (v/v) trichloroacetic acid and kept at  $-20^\circ\text{C}$  for at least 30 min prior to centrifugation at  $4^\circ\text{C}$ . The precipitated proteins were rinsed 3 times with pre-chilled 100% acetone, and then dried at room temperature briefly. The precipitated protein samples were resuspended in the sample buffer containing 50 mM Tris-HCl pH 6.8, 2% (w/v) SDS, 10% (v/v) glycerol, 1% (v/v)  $\beta$ -mercaptoethanol, 0.02% (w/v) bromophenol blue, and denatured by incubating in boiling water for 3 min. Gels were visualized by *InstantBlue Protein* staining (*Expedeon*, USA).

Anti-PsaA (*Agrisera cat. No. AS06172*) and anti-PsbA (*Agrisera cat. No. AS05084*) were applied for monitoring the purities of isolated PSI complexes.

**Peptide LC-MS/MS:** The polypeptide bands of interest from SDS-PAGE were excised and digested by in-gel trypsin (12 ng  $\mu\text{l}^{-1}$  in 25 mM ammonium bicarbonate) overnight at  $37^\circ\text{C}$ . Tryptic peptide fragments were purified by *ZipTip* C-18 tips (*Millipore, Germany*) and the eluted peptide samples were diluted in 0.1% (v/v) formic acid before loading to a *Triple TOF 6600 System* (*ThermoFisher*) mass spectrometer for LC-MS/MS. To avoid carry over contamination, a blank run was inserted between the samples. The data were analyzed using *Analyst TF 1.7.1* software (*Applied Biosystems*) and searched in *Mascot* (*Matrix Science, UK*) against the National Center for Biotechnology Information (NCBI) database and the local *H. hongdechloris* genome sequence draft (unpublished, NCBI SUB897144: LAZT00000000).

**P700:** WL-PSI and FR-PSI complexes were resuspended in 50 mM Tris-HCl (pH = 8.8) containing 0.05% *Triton X-100* at the final Chl concentration of  $\sim 15 \mu\text{g ml}^{-1}$ . Then, 0.33  $\mu\text{M}$  N,N,N',N'-tetramethyl-*p*-phenylenediamine (TMPD) and 0.33  $\mu\text{M}$  potassium ferricyanide were added to the PSI samples and mixed well. The absorbance spectrum was recorded from 650–750 nm. The spectra were then rescanned after adding 6.7  $\mu\text{M}$  ascorbic acid. The P700 spectrum was obtained by subtracting the spectrum recorded prior and after adding ascorbic acid (oxidized – reduced). The concentration of P700 was estimated using a molar extinction coefficient of  $70 \times 10^3$  [L mol<sup>-1</sup> cm<sup>-1</sup>] (Hiyama and Ke 1972) at its maximum absorption peak around 700 nm.

colour due to the presence of orange Chl–protein complexes, which are absent from *H. hongdechloris* samples. Based on absorption spectral analysis and P700 measurement (Fig. 1B), dark green band 2 from the solubilized thylakoid membranes was identified as being enriched in PSI components. Band 1 showed an absorption peak around 672 nm, which was blue-shifted compared to that of band 2, where an absorption peak of 678 nm was

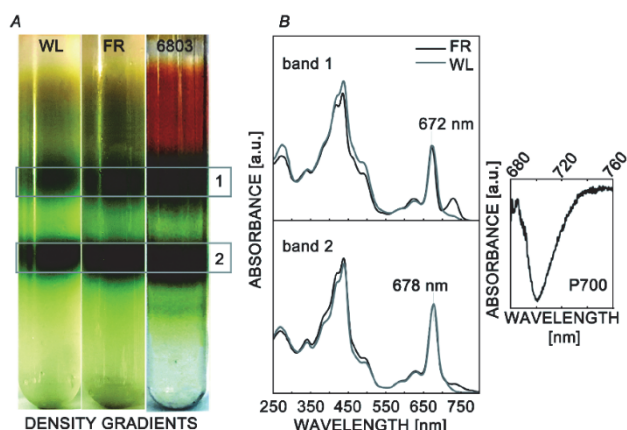


Fig. 1. Purification of PSI complexes. Sucrose density gradients (A) and their absorption spectra (B). P700 measurement of FR-2 band was inserted. WL, white light illumination culture condition; FR, 730 nm LED illumination culture conditions; 6803 represent *Synechocystis* 6803 as a control.

observed (Fig. 1B). An additional absorption component centered at  $\sim 735$  nm was observed from both FR bands (FR-1 and FR-2) (Fig. 1B). Pigment composition analysis indicated that Chl *f* is only detected from FR samples (Fig. 1S), with  $12.0 \pm 0.1\%$  for Chl *f* to total Chl for FR-1 and  $8.4 \pm 0.4\%$  Chl *f* to total Chl for FR-2, which is consistent with absorption spectra presented in Fig. 1B. In addition, much higher pheophytin *a* was observed in the band 1 fractions (WL-1 and FR-1) from *H. hongdechloris*, suggesting that the band 1 is the enriched PSII fraction (Fig. 1S).

The PSI-complex enriched band 2 was further purified on an anion exchange column (*Mono Q<sup>TM</sup> 5/50 GL*) eluting with a gradient of  $\text{MgSO}_4$  (5–200 mM) in 50 min and the major fraction (F-2, Fig. 2A) was collected at the retention time of  $\sim 29$  min with  $\text{MgSO}_4$  concentration of  $\sim 116$  mM. After concentrating the F-2 fractions, highly purified PSI complexes were collected at 9.7 min from *SEC s2000* gel filtration in the buffer A with 0.02% DoDM at the flow rate of  $0.2 \text{ ml min}^{-1}$  (Fig. 2B).

**Polypeptide composition of purified PSI:** The polypeptide composition of isolated PSI complexes was analyzed by SDS-PAGE and Western blotting (Fig. 3). Purified PSI complexes from *Synechocystis* 6803 showed a typical peptide pattern with PsaA and PsaB peptides located above the molecular mark of  $\sim 50$  kDa and visible PsaD, PsaE, PsaC, and PsaK located below 17 kDa, which agrees well with previous reports (Rögner *et al.* 1990, Kruij *et al.* 1993). Purified WL-PSI complexes from WL cultured *H. hongdechloris* cells showed similar peptide patterns as that isolated from FR *H. hongdechloris* cells, but some differences were noticed at the region between  $\sim 10$ –17 kDa. An additional peptide at  $\sim 13$  kDa from WL-PSI complexes (band W5) was identified as PsaL2, while PsaL1 was detected from FR-PSI complexes at  $\sim 17$  kDa position

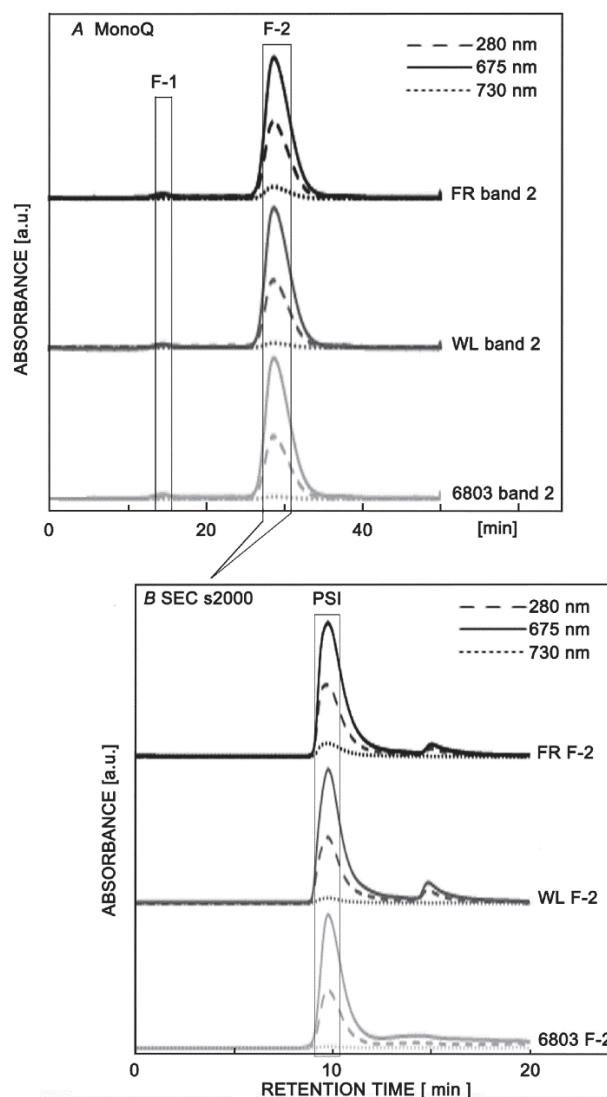


Fig. 2. PSI complexes purification. Elution profile on an anion exchange column (*Mono Q<sup>TM</sup> 5/50 GL*) (A) of sucrose gradient band 2 with flow rate of  $0.8 \text{ ml min}^{-1}$ , and elution profile on a HPLC gel-filtration column (*SEC s2000*) (B) with a flow rate of  $0.2 \text{ ml min}^{-1}$ . Chromatographic profiles were recorded at 280 nm (dashed line), 675 nm (solid line), and 730 nm (dotted line). WL, white light illumination culture condition; FR, 730 nm LED illumination culture conditions; 6803 represent *Synechocystis* 6803 as a control. Black lines are FR samples, grey lines are WL samples, and light grey colored lines are *Synechocystis* 6803 (6803).

(band FR4) (Table 1S). The presence of the PsaL peptide suggested that the purified PSI complexes from *H. hongdechloris* might be in a trimeric form. Additional peptide bands at  $\sim 27$  kDa were observed in the PSI complexes purified from *H. hongdechloris* grown under WL and FR conditions. Western blotting using PsaA antibody revealed two positive bands at  $\sim 50$  and 27 kDa (according to the molecular marker positions), but only one PsaA band was identified from the control, confirming

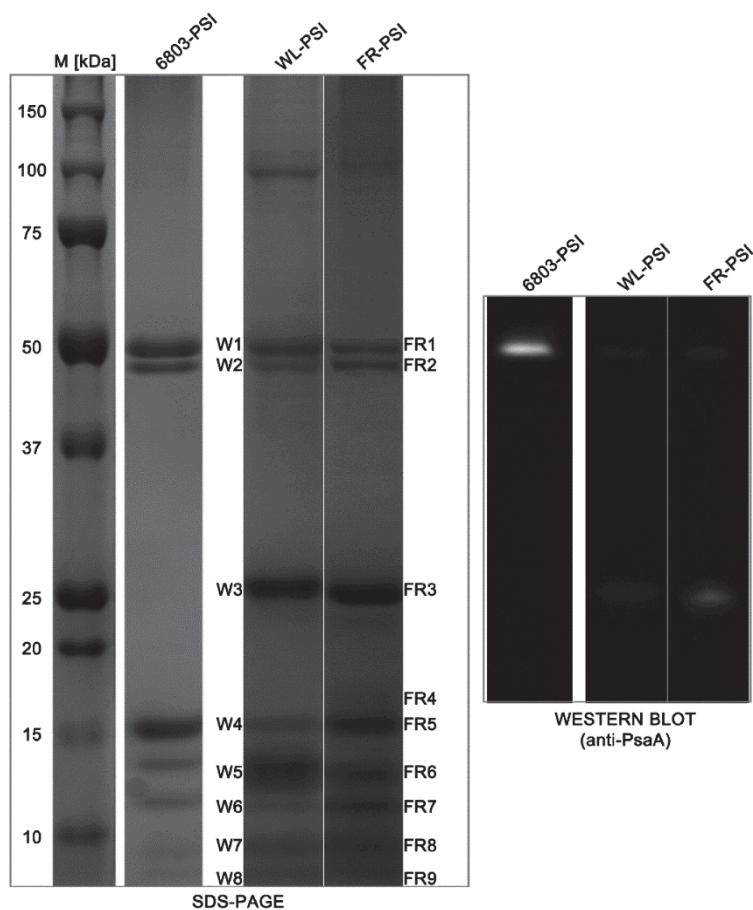


Fig. 3. Polypeptide composition of purified PSI complexes were resolved on a 4–12% Bolt gel and PsaA detection by anti-PsaA. 6803-PSI is purified PSI complexes from *Synechocystis* 6803; WL-PSI is purified PSI complexes from *Halomicronema hongdechloris* cells grown under white light culture condition; FR-PSI is purified PSI complexes from *H. hongdechloris* cells grown under far red light culture condition. Peptides of interest were listed as W1–W8 and FR1–FR9, which were excised for further LC MS/MS measurement (Table 1S).

that the unexpected bands of W3 and FR3 resolved from purified PSI complexes of *H. hongdechloris* were the fragmented PsaA (Fig. 3). Further LC-MS/MS analysis confirmed bands W1 and FR1 are PsaA, while W2 and FR2 are PsaB. W3 and FR3 showed the full coverage of the same peptides of PsaA and PsaB as detected at ~50 kDa (Table 1S). The fragmented PsaA and PsaB located at ~27 kDa were absent in the purified PSI from *Synechocystis* 6803, supporting the conclusion that the fragmented PsaA and PsaB peptides at ~27 kDa are a unique feature for PSI complexes isolated from *H. hongdechloris*. Anti-PsaA (the core of the PSII peptide) was applied on Western blots and negative responses confirmed that isolated PSI complexes are free of PSII contaminations. The LC-MS/MS data confirmed that different *psaA* and *psaB* gene-encoding products are observed in FR-PSI from WL-PSI complexes although the isolated PSI showed that a similar size eluted at ~9.8 min using *SEC s2000* (Fig. 2B). WL-PSI complexes contained PsaA2, PsaB2, PsaF2, and PsaL2. In contrast, the FR-PSI complexes contained PsaA1, PsaB1, and PsaF1, together with PsaL1 and PsaL2, which are located in the gene cluster as “FaRLip” regulation (Li *et al.* 2016). Both FR- and WL-PSI share the same gene products of PsaD, PsaE, PsaC, and PsaK.

**Pigment composition and P700 determination:** The

pigment composition analysis showed that WL-PSI complexes have an almost identical absorption spectrum as that of *Synechocystis* 6803 PSI (6803-PSI) complexes (Fig. 4A), although an oxidized Chl *a*-like component (7 and 4% to Chl *a*, respectively) was only detected in PSI complexes isolated from *H. hongdechloris* (peak X in Fig. 4B). A shoulder centered at ~735 nm was observed from FR-PSI complexes (Fig. 4A), and further HPLC analysis revealed that Chl *f* made up ~8% of total Chl in the FR-PSI complexes with a Chl *a*/Chl *f* ratio of ~12. The  $\beta$ -carotene to Chl *a*' ratio was approximately 26.5 and 34.5 for WL-PSI and FR-PSI, respectively (Fig. 4B). There was no detectable amount of pheophytin *a* in any purified PSI complexes (Fig. 4B). Taken together with the results from the SDS-PAGE, LC-MS/MS peptide analysis, and pigment compositions, the purity of isolated PSI complexes was confirmed.

The spectra of the P700 were determined by chemical difference spectra (Fig. 5). The different spectra of the absorption change between the oxidation and reduction process revealed a clear negative peak at 699 nm for WL-PSI complexes and 702 nm for FR-PSI complexes. P700 measurement confirmed that Chl *a* is a PSI reaction center Chl involved with charge separation. The Chl *f* absorption peak is 707 nm in 100% methanol, therefore, it is impossible for Chl *f* to function as the special pair of Chl

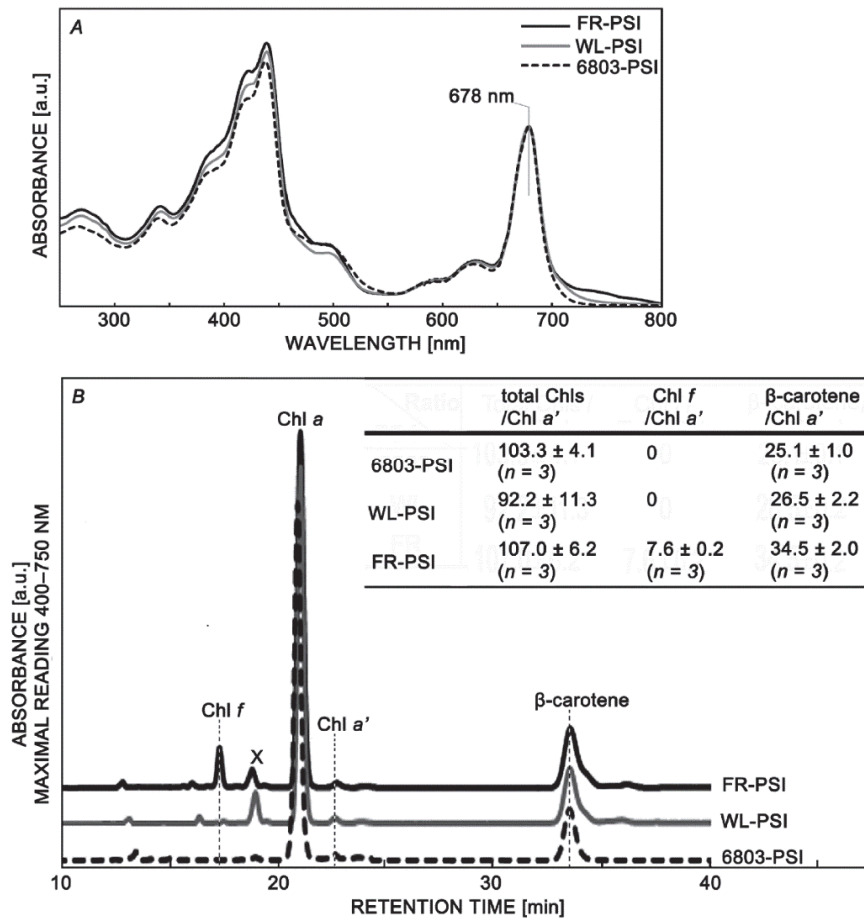


Fig. 4. Absorption spectra of purified PSI complexes (A) and their pigment composition (B). 6803-PSI is purified PSI complexes from *Synechocystis* 6803; WL-PSI is purified PSI complexes from *Halomiconema hongdechloris* cells grown under white light culture condition; FR-PSI is purified PSI complexes from *H. hongdechloris* cells grown under far red light culture condition. Solid black line is purified FR-PSI; solid grey line is purified WL-PSI; and dashed grey line is purified 6803-PSI. The absorption spectra were normalized at chlorophyll (Chl) *a* peak (678 nm) and the HPLC chromatographs were normalized at Chl *a* peak at about 19 min. Chl *f*, Chl *a*, Chl *a*' and  $\beta$ -carotene are assigned based on their retention time and online spectra. An oxidized Chl *a*-like component (peak X) was only detected in PSI complexes isolated from *H. hongdechloris*. The ratios presented in the inserted table are calculated based on the HPLC peak area and their coefficient numbers.

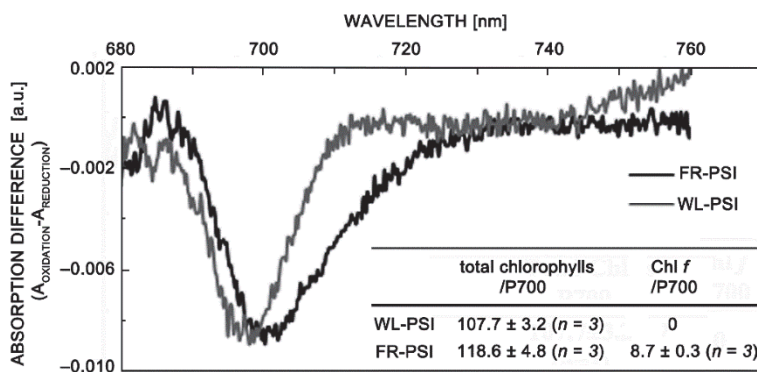


Fig. 5. P700 measurement of purified PSI complexes from *Halomiconema hongdechloris* cells grown under white light (WL-PSI, solid grey line) and far red light (FR-PSI, solid black line). The ratios presented in the inserted table are calculated based on the absorption spectra and their coefficient numbers.

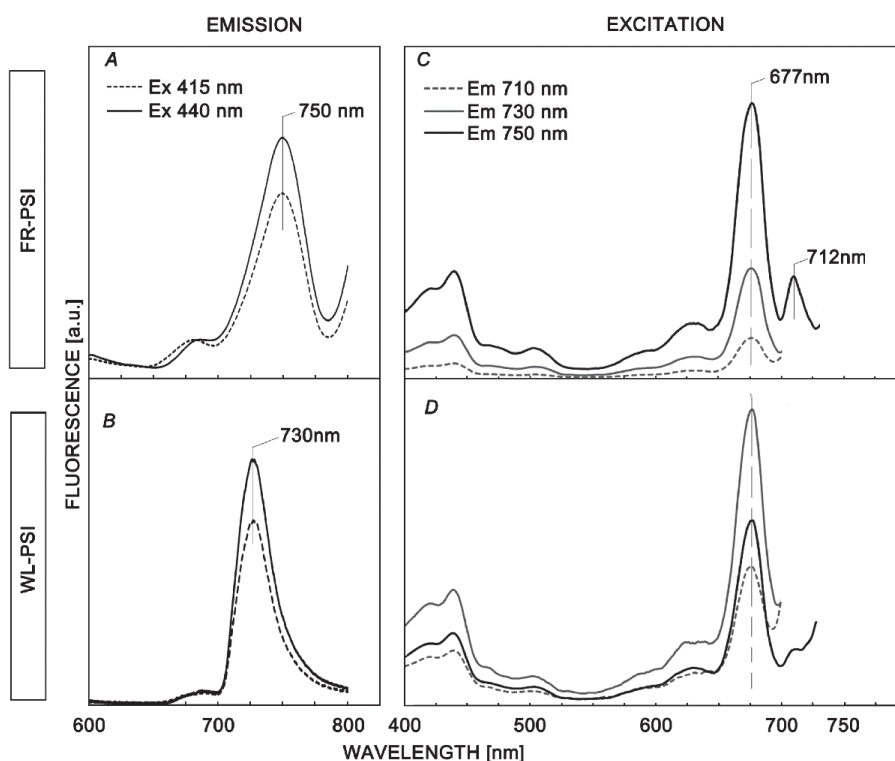


Fig. 6. Low-temperature (77 K) fluorescence spectral analysis of purified PSI complexes from *Halomicronema hongdechloris* cells grown under white light (WL-PSI) and far red light (FR-PSI). (A) Steady-state fluorescence emission spectral comparison using excitation (Ex) wavelength of 415 nm (dashed line) and 440 nm (solid line); (B) Steady-state fluorescence excitation spectral comparison using emission (Em) wavelength of 710 nm (dashed line), 730 nm (grey solid line), and 750 nm (black solid line).

in the isolated PSI complexes. A three nm shift was noticed between WL-PSI and FR-PSI, which could be attributed to the presence of Chl *f* in FR-PSI, although the location and function of Chl *f* is uncertain to date.

In order to estimate the concentration of P700, the molar extinction coefficient of  $70 \times 10^3$  [L mol<sup>-1</sup> cm<sup>-1</sup>] at 701 nm for PSI particles of *Anabaena variabilis* (Hiyama and Ke 1972) was used to estimate the concentration of P700 at 699 nm and 702 nm for WL-PSI and FR-PSI complexes from *H. hongdechloris*. The results indicate that  $107.7 \pm 3.2$  Chl *a*/P700 was determined in WL-PSI compared with  $118.6 \pm 4.8$  Chl *a+f*/P700 determined in FR-PSI. In FR-PSI,  $110.0 \pm 4.4$  Chl *a*/P700 and  $8.7 \pm 0.43$  Chl *f*/P700 were calculated.

To explore the potential function of Chl *f* in isolated FR-PSI, fluorescence spectral analyses were carried out (Fig. 6). The emission fluorescence profiles for WL-PSI and FR-PSI complexes were clearly distinguishable. When PSI particles were excited at 440 nm, a major fluorescence emission band at 730 nm was observed from WL-PSI complexes (Fig. 6A,B), which resembles other isolated Chl *a*-PSI complexes in cyanobacteria (Nyhus *et al.* 1992). FR-PSI complexes showed a major fluorescence emission peak at 750 nm using excitation wavelengths at 415 nm or 440 nm (Fig. 6A,B). The noticeably different pigment composition in FR-PSI could be attributed to the red-

shifted maximal fluorescence, although Chl *f* is only a minor pigment (only about 8% of total Chl). The spectra were almost identical using an excitation wavelength of 415 nm (Soret band of Chl *f*) and 440 nm (Soret band of Chl *a*), except much reduced intensity was observed when excited at 415 nm (Fig. 6A,B). Interestingly, the relative reduced intensities caused by excitation wavelength of 415 nm and 440 nm are negligible between WL-PSI and FR-PSI.

The fluorescence excitation spectra using an emission wavelength of 730 and 750 nm revealed a major peak centered at 677 nm for both WL-PSI and FR-PSI complexes (Fig. 6C,D). However, the intensities of excitation peaks are different. In WL-PSI, the highest excitation 677 nm peak was observed using an emission wavelength of 730 nm, while, the highest excitation 677 nm peak was obtained by emission at 750 nm, which agrees well with fluorescence emission spectra. There are two pigment pools in isolated FR-PSI complexes, 677 nm from Chl *a* and 712 nm from Chl *f*. Using an emission wavelength of 730 nm, no 712-nm peak was observed, suggesting that the Chl *f* pool at 712 nm contributes to 750 nm fluorescence emission. In contrast, there was strong fluorescence recorded from FR-PSI particles at 712 nm compared with only a tiny peak resolved at 706 nm that was observed in the spectrum for WL-PSI particles (Fig. 6C,D).

1JB0_A	1	MTISPFEREFKVRVVDNDPVPTSFEKWKAPGHFDRTLARGPQTTTWIWNLHALAHDFDHTSDLEDISR	70
PsaA_1	1	MTTSPEFQRQRVRVEVDQNPNTSFEKWKAPGHFERSLARGPKTTTWIWDLHADAHDFDSHTDLEDISR	70
PsaA_2	1	MTISPFEPGRKVKVVDSDPVNTSFERWAKPGHFERSLSKGPKTTTWIWDLHADAHDFDSHTSDLEDISR	70
1JB0_A	71	KIFSAPFGHLAVVFIWLSGMYFHGAKFSNYEAWLADPTGIKPSAQVWVPIVGGILNGDVGGGFHGIQIT	140
PsaA_1	71	KIFSAPFGHLAVIFLWLSGMYFHGARFSNFSWMTDPIHIKPSAQVWVPIFGQELNADMGDFRGIQIT	140
PsaA_2	71	KIFSAPFGHLAVIFLWLSGMYFHGAKFSNYEAWLSNPTGIKPSAQVWVPIFGQELNADMGDFRGIQIT	140
1JB0_A	141	SGLFQLWRASGITNEFQLYCTAIGGLVMAGLMLFAGWFHYHKRAPKLEWFQNVESMLNHLHLAGLLGLGSL	210
PsaA_1	141	SGLFQMRWREGGFTHEFQLFWTAIGALVMAALMMFAGWFHYHVRAPKLDWFRNWESMMNHLHLAGLLGLGSL	210
PsaA_2	141	SGLFQMRWRANGITNSFELYCTAIGALVMAAGLMLFAGWFHYHKKAPKLEWFQNVESMMNHLHLAGLLGLGCL	210
1JB0_A	211	AWAGTQIHVSLSLPINKLLDAGVAAK-----DIPLPHEFILNPSLMAELYPKVDWGFSGVIFP	267
PsaA_1	211	GWAGELIHVALPTNKLDDAGVPLE-----DIPLPHEFILNKSIMVDLYP----SFAEGVKPFP	263
PsaA_2	211	GYAGQOIHVSLSLPINACLAIDAGKPLTVGGKVIDSVAIPLPHEWILNPSLMTDIYP----SFAEGLKPF	276
1JB0_A	268	FTFNWAAYSDFLTFENGGLNPNVTGGWLSDTAHHHLAIAVLFIIAGHYMYRTNWGICHSLKEILEAHKGF--	335
PsaA_1	264	FTLNWSAYADFLTFKGGGLNPNVTGGWLMDTAAHHHLVAIAVLFIIAGHYMYRTNWGICHSFRELLDDARTPKM	333
PsaA_2	277	FTLNWSYADFLTFENGGLNPNVTGGWLMDTAAHHHLAIAVLFIVAGHYMYRTNWGICHSPKEVLEAHKGF--	344
1JB0_A	335	-----FTG-AGHKLGLYEVLTTSWHAQLAINLAMGSLSIIVAQHMYAMPPYPYLATDYPTQLSFTTHMW	399
PsaA_1	334	LPIFNFIGVGHRLDKIFETSWHANLAIHLVQFGTASLLVAHMYAMPPYPYLATDYATVTSLFTTHVW	403
PsaA_2	344	-----VTG-EGHKGMYEIFTTSWHCQLSWNLAWIGSLSILVAHMYSMPPYPYIATDYPTQLSFTTHMW	408
1JB0_A	400	IGGFLLVVGGAHGAIFMVRDYPAMNQNNVLDRLRHRDAIISHLNWVCIFLGFHSFGLYVHNDTMRAFG	469
PsaA_1	404	IAGFCIVGGAHAAIFLVRDYNPADHVNVLDRTRHRDTRVVSLLAWVCQFLGFHSFAMYCHNDTMRAFG	473
PsaA_2	409	IGGFLLVVGGAHAAIFMVRDYPATHINLLDRVIRHRDAIISHLNWVCIFLGFHSFGLYVHNDTMRAFG	478
1JB0_A	470	RPQDMFSDTGIQLQVFVAQWVQNLHFLAPGG-----IAPNAAATASVAFG	514
PsaA_1	474	RPQDMFSDTGIQLQPIFAQWVQIQTMVAGANLQAAEPLGNVFGGLRNIDLAVGVVAPLGGFVSHAFG	543
PsaA_2	479	RPQDMFSDTGIQLQVFVAQWVQNLHAAAAG-----IAPNAAAGVSPAFG	523
1JB0_A	515	GDVVAVGGKRAMPEIVLGTADFVHHIHAFTIHTVTVLILLKGVLFARSSRLIPDKANLGRFPDGGPGRG	584
PsaA_1	544	GGVVAIGDKIAMPIQLGTADFLIHHIHAFTIHTVTVLVLLKGVLFARNSRLIPDKGELGFRFPDGGPGRG	613
PsaA_2	524	GDILAVVGGKRAMPEITLGTADFVHHIHAFTIHTVTVLILLKGVLFARNRSLIPDKGELGFRFPDGGPGRG	593
1JB0_A	585	GTCQVSGWDHVFLGLFWMYNCISVVFHFWSWQSDVWGTVPDGTVSHITGGNFAQSAITINGWLRDFL	654
PsaA_1	614	GTCQVSAWDHVFLGLFWMYNSLSIVIFHFWSWQSDVWGTVGDGTISHITGGNFAQASITNNGWLRDFL	683
PsaA_2	594	GTCQVSGWDHVFLGLFWMYNSLSIVIFHFWSWQSDVWGSVSPDGSVSHITAGNFAQSAITINGWLRDFL	663
1JB0_A	655	WAQASQVIGSYGSALSAYGLLFLGAHFFVWAFSLHFLFSGRGYWQELIESIVWAHNLKLVAPAIQPRALSI	724
PsaA_1	684	WAQASQVIGSYGSALSAYGLFFLAGHFFIFGFSLHFLFSGRGYWQELIESIVWAHNLKLVKITTAIQPRALSI	753
PsaA_2	664	WAQASQVIGSYGSALSAYGLLFLGAHFFVWAFSLHFLFSGRGYWQELIESIVWAHNLKLVAPAIQPRALSI	733
1JB0_A	725	IQGRAVGVAFHLLGGIATTWAFFLARIISVG	755
PsaA_1	754	TQGRAVGVAFHLLGGIVTTWAFFLARMAAIG	784
PsaA_2	734	TQGRAVGVAFHLLGGIATTWAFFLARIIAVG	764

Fig. 7. Sequence alignment for PsaA's detected from isolated PSI complexes of *Halomicronema hongdechloris*. PsaA (1JB0\_A) from PSI crystal structure of *Synechococcus elongates* is used as reference. The residues ligating chlorophyll *a'* are in white fonts on a black background. Black squares are conservative chlorophyll-binding residues where two different amino acids were found. (+) represents the residue binding P700. Asterisk (\*) represents the ligation position for the Fe-S clusters. The grey box highlights the extended sequence found in PsaA1. PsaA1 is PsaA peptide detected from FR-PSI complex and PsaA2 is a PsaA peptide detected in the WL-PSI complex.

## Discussion

Purification of PSI is an essential step toward characterization of Chl functions in PSI. The purification of PSI was achieved using a combination of three protein-separation methods. The lack of pheophytin *a* detected from both isolated PSI samples indicates that WL-PSI and FR-PSI samples are free of PSII contamination, which was further confirmed by negative Western blots using anti-PsbA.

Two different PsaL peptides were detected in WL-PSI and FR-PSI. LC-MS/MS analysis confirmed that they are products of different encoded genes. The presence of PsaL in WL-PSI and FR-PSI and their size as shown in the sucrose density gradient, suggested that the isolated PSI complexes from *H. hongdechloris* might be in their

trimeric form, which is different from the previous report that the trimer of the PSI did not exist in FR-grown *Leptolyngbya* JSC-1 (Gan *et al.* 2014).

PSI complexes isolated from FR-*H. hongdechloris* cells contains PsaA1, PsaB1, PsaF1, and PsaL1 and PsaL2, these five subunit encoded genes are located in the gene cluster named as "FaRLip" (Gan *et al.* 2014), which are next to the genes encoding red-shifted phycobilisomes (Li *et al.* 2016). Most subunits showed similar molecular masses, for example PsaA1 is 87 kDa and PsaA2 is 84 kDa (Fig. 7). However, PsaL1 contains 189 Aa (~20 kDa), 30 extra Aa at both terminals of the sequence compared to PsaL2 of 17 kDa (Fig. 2S). PsaL2 was detected from FR-PSI complexes (band FR7 in Fig. 3), however, the



counterpart of PsaI could not be detected in isolated WL-PSI, which may be due to the small size or smaller amount of the proteins. PsaL and PsaI play important roles in trimeric PSI construction in cyanobacteria (Grotjohann and Fromme 2005). The switched PSI subunits including PsaL1 and PsaL2 might indicate the changed structure of FR-PSI compared with WL-PSI, which may be in relation to the replacement of Chl *f* in FR-PSI. Further structural investigation is needed. However, the isolated WL-PSI and FR-PSI are similar in size based on the band positions located in the sucrose gradients and the identical retention time on SEC *s2000* separation. The amino acids surrounding the special pair of Chls are identical and most Chl-associated ligands are conserved (highlight in a sequence comparison in Fig. 7). Two out of three different amino acid substitutions at Chl-binding sites of PsaA1 and PsaA2 are His and Gln conservative substitution, suggesting no functional changes. However, there is Ala at the site of 328 in PsaA1, instead of His in PsaA2, which may result in the loss of Chl-binding ability (Fig. 7). An extension sequence in PsaA1 is noticed. Further functional investigation is required.

The isolated FR-PSI complexes contains ~107 Chl (including 8 Chl *f*) per Chl *a'*, while WL-PSI contains

~92 Chl per Chl *a'* (Fig. 4B). This is similar to the results from P700 (Fig. 5). There are ~119 Chl (including 9 Chl *f*) per P700 in isolated FR-PSI and 108 Chl per P700 in isolated WL-PSI. Chl *f* in FR-PSI seems to function as an additional accessory Chl, as there are 99 Chl *a* per Chl *a'* or 110 Chl *a* per P700. This is similar to the Chl *a* ratio in WL-PSI, which does not contain Chl *f*. However, Chl *f* in FR-PSI contributes to the red-shifted emission fluorescence of 750 nm and influences the red-shifted reaction center special Chl *a*, resulting in P702 instead of the P699 found in WL-PSI.

In this study, we isolated and purified the PSI from *H. hongdechloris* grown under FR- and WL-light conditions. The size of the isolated PSI complexes was identical for these two culture conditions, but some peptides in the FR-PSI are the products of different genes, which are associated with FR regulation and the phenomena of "FaRLip". Chl *a* is the major PSI reaction center Chl, but a slight absorption shift is observed in FR-PSI from WL-PSI, which may be due to protein environmental changes or the involvement of Chl *f* in FR-PSI. The chlorophylls per each PSI were similar in FR-PSI and WL-PSI complexes, except the additional 8 Chl *f* found in the FR-PSI complexes.

## References

- Airs R.L., Temperton B., Sambles C. *et al.*: Chlorophyll *f* and chlorophyll *d* are produced in the cyanobacterium *Chlorogloeopsis fritschii* when cultured under natural light and near-infrared radiation. – *FEBS Lett.* **588**: 3770-3777, 2014.
- Akutsu S., Fujinuma D., Furukawa H. *et al.*: Pigment analysis of a chlorophyll *f*-containing cyanobacterium strain KC1 isolated from Lake Biwa. – *Photochem. Photobiol.* **33**: 35-40, 2011.
- Amunts A., Toporik H., Borovikova A. *et al.*: Structure determination and improved model of plant photosystem I. – *J. Biol. Chem.* **285**: 3478-3486, 2010.
- Barber J.: Photosynthetic generation of oxygen. – *Philos. T. R. Soc. B* **363**: 2665-2674, 2008.
- Barth P., Lagoutte B., Sétif P.: Ferredoxin reduction by photosystem I from *Synechocystis* sp. PCC 6803: toward an understanding of the respective roles of subunits PsaD and PsaE in ferredoxin binding. – *Biochemistry* **37**: 16233-16241, 1998.
- Ben-Shem A., Frolow F., Nelson N.: Crystal structure of plant photosystem I. – *Nature* **426**: 630-635, 2003.
- Chen M., Blankenship R.: Expanding the solar spectrum used by photosynthesis. – *Trends Plant Sci.* **16**: 427-431, 2011.
- Chen M., Li Y., Birch D. *et al.*: A cyanobacterium that contains chlorophyll *f* – a red-absorbing photopigment. – *FEBS Lett.* **586**: 3249-3254, 2012.
- Chen M., Schliep M., Willows R. *et al.*: A red-shifted chlorophyll. – *Science* **329**: 1318-1319, 2010.
- Croce R., van Amerongen H.: Light-harvesting in photosystem I. – *Photosynth. Res.* **116**: 153-166, 2013.
- El-Khouly M.E., El-Mohsnawy E., Fukuzumi S.: Solar energy conversion: From natural to artificial photosynthesis. – *J. Photoch. Photobio. C* **31**: 36-83, 2017.
- El-Mohsnawy E., Kopczak M.J., Schlodder E. *et al.*: Structure and function of intact photosystem I monomers from the cyanobacterium *Thermosynechococcus elongatus*. – *Biochemistry* **49**: 4740-4751, 2010.
- Fromme P., Jordan P., Krauß N.: Structure of photosystem I. – *BBA-Bioenergetics* **1507**: 5-31, 2001.
- Gan F., Bryant D.A.: Adaptive and acclimative responses of cyanobacteria to far-red light. – *Environ. Microbiol.* **17**: 3450-3465, 2015.
- Gan F., Zhang S., Rockwell N.C. *et al.*: Extensive remodeling of a cyanobacterial photosynthetic apparatus in far-red light. – *Science* **345**: 1312-1317, 2014.
- Golbeck, J.H.: Photosystem I in cyanobacteria. – In: Bryant D.A. (ed.): *The Molecular Biology of Cyanobacteria*. Pp. 319-360. Springer, Dordrecht 1994.
- Golub M., Hejazi M., Kölsch A. *et al.*: Solution structure of monomeric and trimeric photosystem I of *Thermosynechococcus elongatus* investigated by small-angle X-ray scattering. – *Photosynth. Res.* **133**: 163-173, 2017.
- Goodwin W.: Biochemistry of pigments. – In Waterman T.H. (ed.): *The Physiology of Crustacea*. Pp. 101-140. Academic Press, New York and London 1960.
- Grotjohann I., Fromme P.: Structure of cyanobacterial photosystem I. – *Photosynth. Res.* **85**: 51-72, 2005.
- Hiyama T., Ke B.: Difference spectra and extinction coefficients of P 700. – *BBA-Bioenergetics*. **267**: 160-171, 1972.
- Hou H.J., Allakhverdiev S.I., Najafpour M.M. *et al.*: Current challenges in photosynthesis: from natural to artificial. – *Front Plant Sci.* **5**: 232, 2014.
- Hu Q., Miyashita H., Iwasaki I. *et al.*: A photosystem I reaction center driven by chlorophyll *d* in oxygenic photosynthesis. – *P. Natl. Acad. Sci. USA* **95**: 13319-13323, 1998.
- Jordan P., Fromme P., Witt H.T. *et al.*: Three-dimensional structure of cyanobacterial photosystem I at 2.5 angstrom resolution. – *Nature* **411**: 909-917, 2001.
- Kruip J., Boekema E.J., Bald D. *et al.*: Isolation and structural

- characterization of monomeric and trimeric photosystem I complexes (P700. F<sub>A</sub>/F<sub>B</sub> and P700. F<sub>X</sub>) from the cyanobacterium *Synechocystis* PCC 6803. – J. Biol. Chem. **268**: 23353-23360, 1993.
- Li M., Semchonok D.A., Boekema E.J., Bruce B.D.: Characterization and evolution of tetrameric photosystem I from the thermophilic cyanobacterium *Chroococcidiopsis* sp TS-821. – Plant Cell **26**: 1230-1245, 2014.
- Li Y., Cai Z.-L. Chen M.: Spectroscopic properties of chlorophyll *f*. – J. Phys. Chem. B **117**: 11309-11317, 2013.
- Li Y., Chen M.: Novel chlorophylls and new directions in photosynthesis research. – Funct. Plant Biol. **42**: 493-501, 2015.
- Li Y., Lin Y., Garvey C.J. *et al.*: Characterization of red-shifted phycobilisomes isolated from the chlorophyll *f*-containing cyanobacterium *Halomicronema hongdechloris*. – BBA-Bioenergetics **1857**: 107-114, 2016.
- Li Y., Lin Y., Loughlin P. *et al.*: Optimization and effects of different culture conditions on growth of *Halomicronema hongdechloris* – a filamentous cyanobacterium containing chlorophyll *f*. – Front. Plant Sci. **5**: 67, 2014.
- Li Y., Scales N., Blankenship R. E. *et al.*: Extinction coefficient for red-shifted chlorophylls: chlorophyll *d* and chlorophyll *f*. – BBA-Bioenergetics **1817**: 1292-1298, 2012.
- Miyashita H., Ikemoto H., Kurano N. *et al.*: Chlorophyll *d* as a major pigment. – Nature **383**: 402, 1996.
- Mühlenhoff U., Zhao J., Bryant D.A.: Interaction between photosystem I and flavodoxin from the cyanobacterium *Synechococcus* sp. PCC 7002 as revealed by chemical cross-linking. – Eur. J. Biochem. **235**: 324-331, 1996.
- Nelson N., Junge W.: Structure and energy transfer in photosystems of oxygenic photosynthesis. – Annu. Rev. Biochem. **84**: 659-683, 2015.
- Nyhus K.J., Ikeuchi M., Inoue Y. *et al.*: Purification and characterization of the photosystem I complex from the filamentous cyanobacterium *Anabaena variabilis* ATCC 29413. – J. Biol. Chem. **267**: 12489-12495, 1992.
- Ohkubo S., Miyashita H.: A niche for cyanobacteria producing chlorophyll *f* within a microbial mat. – ISME J. **11**: 2368-2378, 2017.
- Rögner M., Nixon P.J., Diner B.A.: Purification and characterization of photosystem I and photosystem II core complexes from wild-type and phycocyanin-deficient strains of the cyanobacterium *Synechocystis* PCC 6803. – J. Biol. Chem. **265**: 6189-6196, 1990.
- Schluchter W.M., Shen G., Zhao J., Bryant D.A.: Characterization of *psaL* and *psaL* mutants of *Synechococcus* sp. strain PCC 7002: a new model for state transitions in cyanobacteria. – Photochem. Photobiol. **64**: 53-66, 1996.
- Sivakumar V., Wang R., Hastings G.: Photo-oxidation of P740, the primary electron donor in photosystem I from *Acaryochloris marina*. – Biophys. J. **85**: 3162-3172, 2003.
- Tomo T., Kato Y., Suzuki T. *et al.*: Characterization of highly purified photosystem I complexes from the chlorophyll *d*-dominated cyanobacterium *Acaryochloris marina* MBIC 11017. – J. Biol. Chem. **283**: 18198-18209, 2008.
- Xu Q., Hoppe D., Chitnis V.P. *et al.*: Mutational analysis of photosystem I polypeptides in the cyanobacterium *Synechocystis* sp. PCC 6803. Targeted inactivation of *psaI* reveals the function of *psaI* in the structural organization of *psaL*. – J. Biol. Chem. **270**: 16243-16250, 1995.
- Xu W., Chitnis P., Valieva A. *et al.*: Electron transfer in cyanobacterial photosystem I: I. Physiological and spectroscopic characterization of site-directed mutants in a putative electron transfer pathway from A0 through A1 to FX. – J. Biol. Chem. **278**: 27864-27875, 2003.